

SYNTHESIS AND CHARACTERIZATION OF SUBSTITUTED GROUP CONTROLLED PYRENE DERIVATIVES WITH RADICAL CATIONS

Shunjie Li^{a,*} and Jian Chen^b^aCollege of Chemistry and Materials Science, Anhui Normal University, 241000 Wuhu – AH, China^bCollege of Chemistry and Materials Science, Huaibei Normal University, 235000 Huaibei – AH, China

Received: 01/06/2024; accepted: 04/10/2024; published online: 06/25/2024

Two novel alkyl thiophene-modified pyrene derivatives (**1**–**2**) were created and synthesized using palladium-catalyzed Stille coupling processes and Friedel-Crafts reaction of pyrene. The polycyclic aromatic groups of the thiophene-modified pyrene were oxidized with $\text{Ag}[\text{Al}(\text{OC}(\text{CF}_3)_3)_4]$ to provide the insensitive radical cations **1**^{•+}–**2**^{•+} based on the alkyl thiophene-modified pyrene derivatives. Nuclear magnetic resonance (NMR), electron paramagnetic resonance (EPR), UV-Vis spectroscopy, and density functional theory (DFT) calculations, were used to investigate their structures and properties. The pyrene moieties were the primary location of the electron spin distribution, with a little overflow onto the outer thiophene moieties. Due to the different substituent groups, free radicals **1**^{•+}–**2**^{•+} exhibit some different properties. Compound **1**^{•+} is the most extensive thiophene-modified pyrene radical cation that has been reported. These species are anticipated to have wide-ranging potential in the areas of optoelectronic materials and semiconductors.

Keywords: thiophene; pyrene; radical; cation; aromatic hydrocarbon.

INTRODUCTION

Due to the potential applications of free radicals in various studies such as inorganic chemistry, organic chemistry, and materials science, people are increasingly interested in free radical chemistry.^{1,2} Organic free radicals are not only powerful synthetic intermediates, but can also serve as emerging functional materials, with the potential to achieve innovative technologies in various fields such as organic magnets, spintronics, optoelectronics, and quantum information.³⁻⁷ Hence, it is imperative to amalgamate unpaired electrons with polycyclic aromatic hydrocarbons, which are extensively employed in organic optics and electronic materials. These compounds have the potential to be utilized in the synthesis of organic light-emitting devices (OLEDs), organic field effect transistors (OFETs), organic photovoltaics (OPVs) materials, and several other functional materials.⁸ In addition, such radicals have a clear tendency toward spin delocalization and can regulate spin coupling and strength through π -orbital distribution.⁹

Pyrene and substituent modified-pyrene derivatives are representative polycyclic aromatic hydrocarbons (PAHs) that exhibit both electron-donating and electron-withdrawing properties. They are primarily utilized as materials with conductivity and light sensitivity. More significantly, because of its tremendous luminescence efficiency, high carrier mobility, superior solution processability, and thermal stability, pyrene has a lot of potential for use in organic light-emitting devices.¹⁰⁻¹³ Pyrene, with its extensive planar conjugated aromatic structure, has a strong inclination towards π -stacking and *quasi*-molecular formation. Every year, there are many literature materials^{14,15} on the substitution of pyrene by various aromatic groups in non-K regions (positions 1, 3, 6, and 8). The in-depth research¹⁶⁻¹⁹ in this field is due to its widespread applications in medicine, chemical sensors, and organic electronics. However, there are relatively few reports on tetrasubstituted pyrenes located in the K-region (4, 5, 9, 10-). The species of radicals after single electron oxidation are rarely reported. Related research²⁰ has demonstrated that by lowering the rotational degrees of freedom in the molecule, bridging sulfur on

thiophene-doped aromatic compounds can efficiently optimize π -orbital overlap. Furthermore, the stability of the compound can be significantly enhanced by the thiophene moiety. Many aromatic compounds modified with thiophene have been created and utilized in organic semiconductor components.²¹⁻²³ Aromatic compounds modified with thiophene have reduced maximum molecular orbital occupancy energy and comparatively wide band gaps. These compounds have sparked a lot of interest in enhancing aromatic stability and increasing π -orbital overlap as potential electronic materials.

Thiophene derivatives undergo significant alterations in their transition intensities and optical energy levels when they are oxidized to form matching cations or radical cations. However, it should be noted that the majority of these cations are not stable. Single radical cations possess distinctive electronic structures and intriguing chemical and magnetic characteristics in comparison to neutral molecules.²⁴ Currently, there is a limited amount of information available on sulfur-containing aromatic radical cations. The distribution of electron spin density is the primary determinant of the physical and chemical characteristics of radicals. Hence, the technique of manipulating the distribution of electron spin density is crucial in acquiring valuable radical entities. Extensive studies²⁵ have been undertaken by researchers to manipulate unpaired electrons using several methods, such as inserting bulky spatial substituents, enlarging π -conjugated systems, and incorporating heteroatoms. In this study, we introduced an alkyl thiophene functional group with high steric hindrance to delocalize and form pairs of electrons throughout the conjugated system. Meanwhile, many interesting conclusions were drawn by comparing the analogs obtained by replacing alkyl with methoxy groups. This article synthesized and characterized for the first time a compound combining alkyl thiophene-modified pyrene (**1**) (Me-TTP) and (**2**) (MeO-TTP) obtained by replacing methyl with methoxy groups. Then, we used $\text{Ag}[\text{Al}(\text{OC}(\text{CF}_3)_3)_4]$ to oxidize **1** and **2** with one-electron, obtaining the corresponding single radical cations and studying their properties. Thiophene-modified pyrene single radicals have distinct electrical structures and intriguing chemical characteristics when compared to neutral precursor molecules. At the same time, the substituent effect that occurs in radicals was discussed. Lastly, we discussed the

*e-mail: huizhanng97@163.com

applications of the novel thiophene-modified pyrene in the fields of optoelectronic materials as well as semiconductors.

EXPERIMENTAL

General methods

All Schlenk approach was used to synthesize air- and water-sensitive chemicals in a glove box under inert atmospheres. Tetrahydrofuran is freshly distilled on Na/benzophenone and degassed three times before use. Dichloromethane is distilled fresh with CaH₂ and degassed three times before use. *N,N*-dimethylformamide uses a 4A molecular sieve to remove water before use. Energy Chemical Co., Ltd. (Shanghai, China) provided all of the commercially available ingredients, and procedures documented in the literature were used to synthesize alkyl thiophene-modified pyrene.

Synthesis of thiophene-modified pyrene (R-TTP)

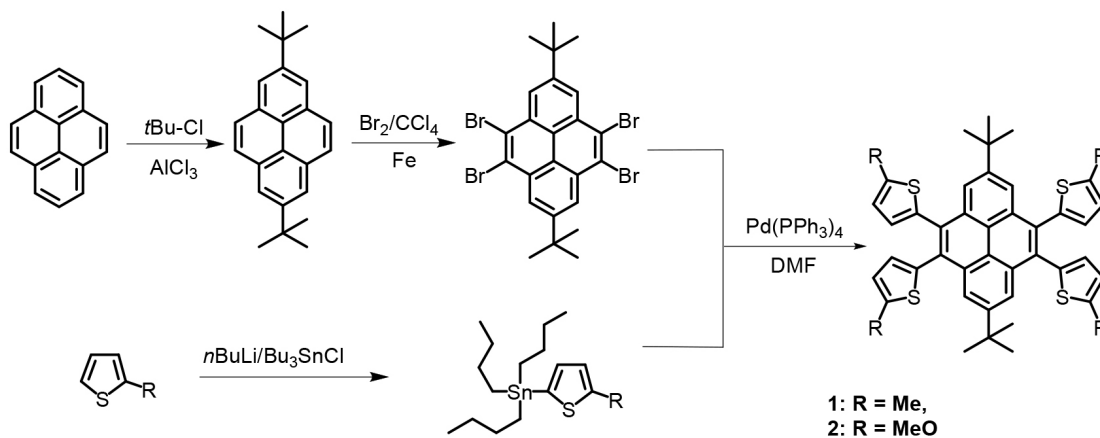
Pyrene finds it easier to conduct an electrophilic substitution process at positions 1, 3, 6, and 8 compared to positions 4, 5, 9, and 10. Instead, these replacements must be completed through indirect electrophilic reaction.²⁶ Using the Friedel-Crafts reaction of pyrene with trimethylchloromethane, *tert*-butyl moieties were first added as protecting groups at positions 2 and 7 of pyrene. Afterward, 2,7-di-*tert*-butylpyrene was brominated using six equivalents of bromine in a solution of carbon tetrachloride with iron powder present. The result was 4,5,9,10-tetrabromo-2,7-di-*tert*-butylpyrene. In the meantime, tributyltin chloride was added to 2-methylthiophene to create 2-(tributyltin)-5-methylthiophene through a lithiation reaction with *n*-butyllithium.^{27,28} An important step in the production of

tert-butyl thiophene-modified pyrene (**1**) was the Stille coupling process between organotin reagent and tetrabromopyrene derivatives using palladium catalyst Pd(PPh₃)₄.²⁹ The compound **2** was also produced by the same process (Scheme 1).³⁰⁻³²

Nuclear magnetic resonance (NMR) spectroscopy was used to evaluate compounds **1** and **2** after they were prepared by Scheme 1. The distinctive signals of methyl and methoxy groups in the ¹H NMR spectra are located at δ 2.37 and 1.41 ppm, respectively. To explain the structural alterations that occur during one-electron oxidation or reduction, we performed quantitative calculations on crystal **1** (Figure 1). The HOMO (highest occupied molecular orbital) and LUMO (lowest unoccupied molecular orbital) of compound **1** were fully delocalized over the pyrene moiety, suggesting that **1** can function as both an electron acceptor and an electron donor simultaneously in this unusual structure. As *per* earlier studies,³³ we discovered that the orbital distribution causes **1** to either gain or lose electrons.

Synthesis of thiophene-modified pyrene radical cations (R-TTP^{•+})

In the presence of nitrogen, compound **1** was subjected to direct treatment with Ag[Al(OC(CF₃)₃)₄] in CH₂Cl₂ for 48 h, resulting in the formation of a dark green solution. After gathering the filtrate, a blackish green powder **1^{•+}**[Al(OC(CF₃)₃)₄]⁻ was produced. After being produced in a modest yield, the monoradical **1^{•+}** was insensitive in room temperature ambient air for over a week. Similarly, the treatment of compound **2** with Ag[Al(OC(CF₃)₃)₄] for 48 h produced a dark red solution. After gathering the red filtrate, a black powder was obtained and identified as monoradical **2^{•+}** (Scheme 2). Monoradicals **2^{•+}** demonstrated stability in ambient air for over 2 weeks at room temperature. Therefore, monoradical cations **1^{•+}** and **2^{•+}** are stable



Scheme 1. Synthesis of the thiophene-modified pyrene R-TTP (**1**) and (**2**)

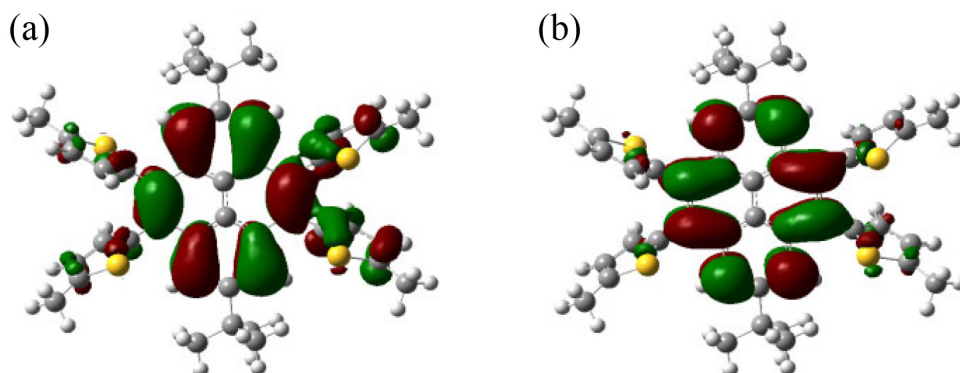
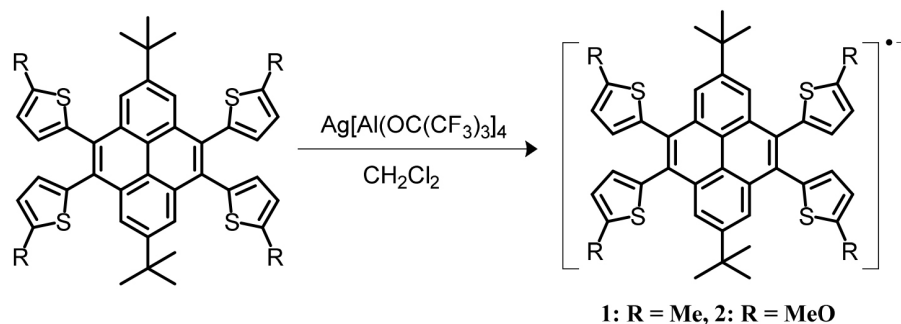


Figure 1. The HOMO (a) and LUMO (b) of **1**



Scheme 2. Synthesis of alkyl thiophene-modified pyrene radical cations R -TTP $^{•+}$ $1^{•+}$ - $2^{•+}$

enough to support us in a series of characterizations. Four alkyl and alkoxy groups were inserted, and this successfully stabilized the free radicals. Interestingly, the color of compound **1** darkened more quickly than the color of compound **2** changed during the process; this could be because the methyl group of compound **1** gave it greater solubility. AgSbF_6 were compared as well, and the same outcomes were found.

Characterization

For compound weighing, a FA2005 electronic analytical balance (T-Bota Sciotech Co., Ltd., Shanghai, China) was employed. A Bruker EMX plus-6/1 instrument (Billerica, USA) was used to record electron paramagnetic resonance (EPR) spectra, which were then simulated using WinEPR Simfonia software. An MPMS-XL7 SQUID (Quantum Design, Beijing, China) was used to measure the magnetic property of a sample that was prepared in a glove box. In a CHI661E chemical workstation glove box, cyclic voltammetry (CV) was used. The counter electrode was platinum wire, and the working electrode was a platinum stick electrode. Element analyses were performed at the University of Science and Technology of China. On silica gel plates (hsf 255), thin-layer chromatography was carried out, and the products of column chromatography were separated on silica gels with a mesh size of 300–400. To integrate the diffraction data and adjust for the effects of polarization and Lorentz, the SAINT software was utilized. For the semi-empirical absorption correction, the SADABS program was utilized. After the crystal structure was solved directly, the full-matrix least-squares method of the Shellxl-2014 crystallographic software program was used to anisotropically refine every non-H atom on F2.

RESULTS AND DISCUSSION

Electrochemical properties

In order to comprehend the charge transfer properties, electrochemical stability, and ionization potential of the substances,

the redox properties of compound **1** were investigated through cyclic voltammetry. According to Figure 2a, the cyclic voltammetry curve of compound **1** showed two *quasi*-reversible oxidation signals (**1**, $E_{1/2}^{\text{ox}} = 1.11, 1.61$ V) at room temperature, suggesting the stability of single cation $1^{•+}$ and double cation 1^{2+} in solution under the conditions of cyclic voltammetry. Because of the high magnitude of the second oxidation potential of $1^{•+}$, conventional oxidizing agents faced challenges in oxidizing this species. Consequently, the production of the double cation 1^{2+} through chemical oxidation proved to be challenging. The initial oxidation potential can be used to estimate the E_{HOMO} value using a cyclic voltammogram.³⁴ For **1**, the $E_{\text{HOMO}} = -5.02$ eV according to the formula: $E_{\text{HOMO}} = -e(E_{\text{ox}} + 4.72)$ (eV). Figure 2b illustrates that $E_{1/2}^{\text{ox}} = 0.95, 1.30$ V, resulting in the calculation of the E_{HOMO} value of **2** as -4.91 eV. The oxidation doping stability of organic semiconductors is associated with their ionization potential, specifically the E_{HOMO} . As a result, in an ambient oxygen atmosphere, decreasing E_{HOMO} and the p -doping level can improve environmental stability. Because it is less likely to be doped with oxygen than the majority of modern OFET materials,³⁵ its relatively low E_{HOMO} level of **1** indicates that it has superior stability to oxidation than conventional p -type semiconductor materials.³⁶

Electronic properties

Obviously, due to the absence of single electron compounds **1** and **2** are EPR-silenced species. The magnetic characteristics of $1^{•+}$ and $2^{•+}$ were investigated through the application of EPR spectroscopy. Initially, a solution of $1^{•+}$ in CH_2Cl_2 was diluted to 10^{-4} M for the EPR test at 298 K. The results showed that there is hyperfine coupling between the hydrogen atom on the pyrene ring and the unpaired electron of $1^{•+}$ (Figure 3a). The g -factor was found to be 2.0032 and the ^1H hyperfine coupling constant to be $A(^1\text{H}) = 3.82$ G, 4H, based on the simulated EPR spectrum. The EPR spectra of a low-temperature solution of $1^{•+}$ were then obtained at 90 K. The single-electron oxidized $1^{•+}$ spectrum displayed diradical features (Figure 3b).

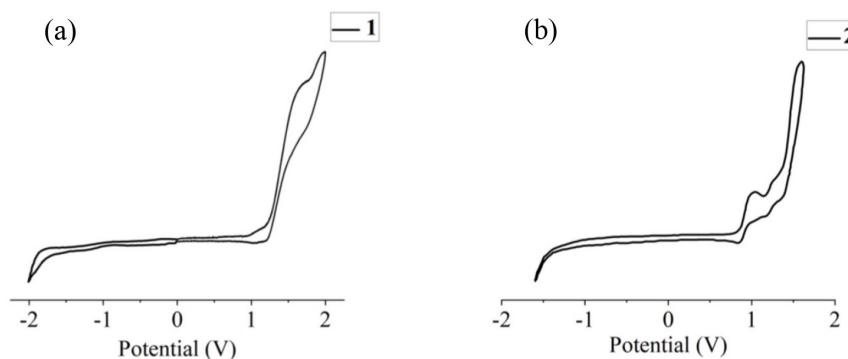


Figure 2. Cyclic voltammetry curve of **1** (a) and **2** (b)

Simultaneously, we detected the half-field forbidden transition signal at low temperatures, which was determined to be $\Delta m_s = \pm 2$. The zero-field splitting value D was obtained as 26.5 G. Additionally, the EPR test of solid powder was examined at 90 K, revealing both a half-field and a diradical signal. As a result, the EPR pattern implied that the central pyrene moiety was the primary location of the cationic charge. Unsurprisingly, the EPR spectrum of 2^{+} yielded results that were comparable to those of 1^{+} . The diradical signal of 2^{+} was successfully detected, and the low-temperature powder EPR spectrum of 2^{+} also showed a significant half-field forbidden transition signal with $\Delta m_s = \pm 2$ (Figure 3c). In contrast to methyl groups, methoxyl groups produce an EPR spectrum with a little broader line width and less obvious splitting of the signal with $\Delta m_s = \pm 1$. These small variations could be explained by the different electrical effects of the methoxy and methyl groups.

X-Ray crystallographic analysis

We collected and analyzed the crystallographic data of compound **1** (Figure 4), crystallized in the triclinic space group P1. Selected bond lengths are shown in Table 1, and the relevant crystal parameters and structural refinement data are provided in Table 1S (Supplementary Material). Due to the addition of the alkyl thiophene group, the central pyrene moiety of the new compound was not completely planar; rather, it was slightly curved. A comparison between the bond length data of **1** and 2,7-di-*tert*-butylpyrene indicated a change in the C–C bond length of the aromatic ring. Upon the addition of thiophene functional groups, the distance

between C6–C7 and the two carbon atoms directly connected to the thiophene functional groups increased from 1.348 to 1.353 Å, and the C7–C13 bond length increased from 1.439 to 1.455 Å. Furthermore, the C13–C14 bond length decreased from 1.399 to 1.388 Å, the C22–C23 bond length decreased slightly from 1.422 to 1.415 Å, and the C13–C22 bond length did not change significantly. These changes were conducive to the generation of radicals and the emergence of diradical signals. Unfortunately, we did not obtain crystallographic data for radical cations 1^{+} and 2^{+} , potentially due to the presence of a residue from the tin reagent. Thus, we could not further investigate the effect of electron loss on the structure of the aromatic skeleton.

DFT calculations

In order to conduct a more in-depth analysis of the electronic characteristics, we conducted quantitative computations of 1^{+} at the (U)m062x/6-31g* level. According to relevant reports,³⁷

Table 1. Selected bond lengths (Å) of compound **1**

Bond lengths / Å	Compound 1	Pyrene
C13–C14	1.388	1.399
C7–C13	1.455	1.439
C6–C7	1.353	1.348
C13–C22	1.415	1.415
C22–C23	1.415	1.422

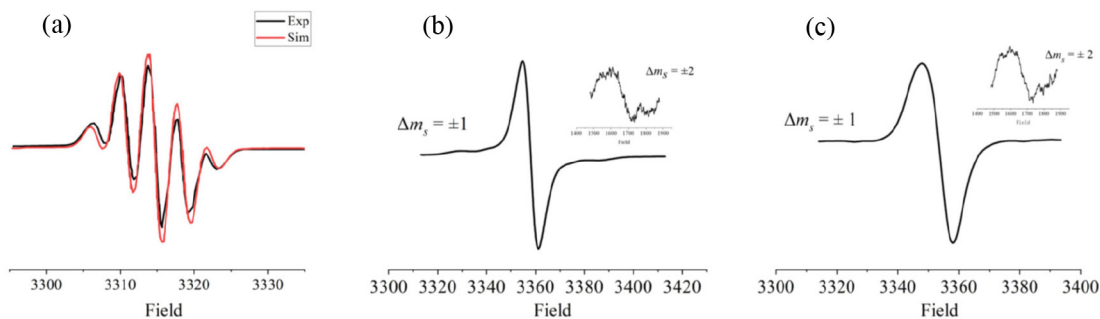


Figure 3. EPR spectrum of (a) 10^{-4} M 1^{+} in CH_2Cl_2 at 298 K; (b) 10^{-4} M 1^{+} in CH_2Cl_2 at 90 K; (c) powder 2^{+} at 90 K

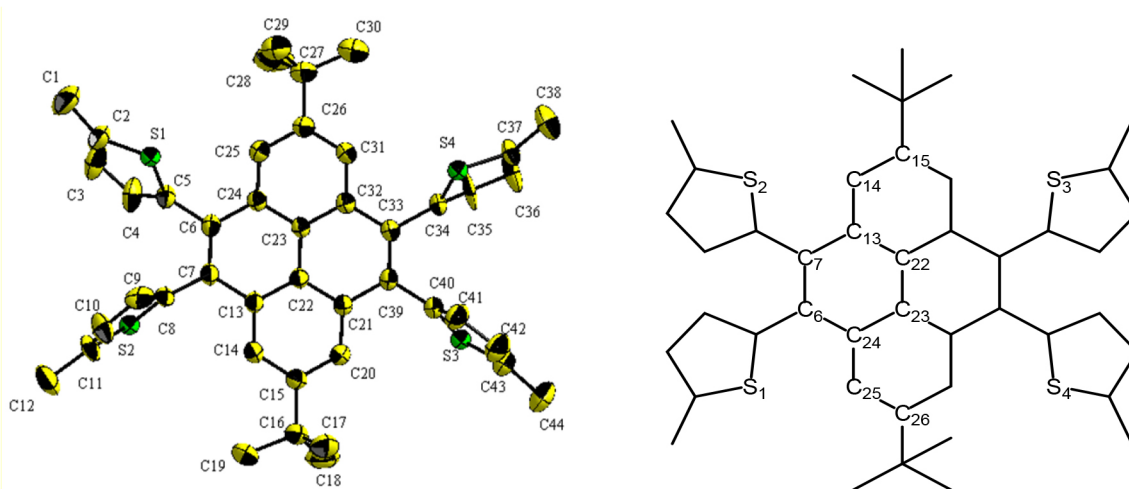


Figure 4. Thermal ellipsoid (50%) drawing of **1**. All hydrogen atoms are not shown for clarity. Selected bond lengths (Å): C13–C14, 1.388(3); C13–C22, 1.415(3); C13–C7, 1.454(3); C32–C31, 1.395(3); C32–C23, 1.417(3); C32–C33, 1.450(3); C14–C15, 1.391(3); C23–C24, 1.414(3); C23–C22, 1.415(3); C21–C20, 1.387(3); C21–C22, 1.422(3); C21–C39, 1.447(3); C20–C15, 1.390(3); C6–C7, 1.353(3); C6–C24, 1.457(3); C25–C24, 1.390(3); C39–C33, 1.357(3); C26–C31, 1.386(3); C26–C25, 1.392(3)

using m062x for geometric optimization is more appropriate, especially in the presence of weak intramolecular interactions and large conjugations. Upon the incorporation of 2-methylthiophene functional groups, it was anticipated that unpaired electrons would be dispersed throughout the entire conjugated system. We attributed this dispersion to the variation in the length of the bond caused by the electron-rich alkyl thiophene group, based on our study of the computational data. The distribution of spin density in $\mathbf{1}^{+\bullet}$, in the lowest unoccupied molecular orbital (LUMO), and the singly occupied molecular orbital (SOMO) extended across the hold molecule, with the spin density being less dispersed on the thiophene ring but notably prominent at the pyrene moiety (see Figures 5a and 5b). The spin densities observed in $\mathbf{1}^{+\bullet}$ indicate that the presence of substituents influences the degree of radical delocalization, thereby influencing the ground states. The electron-donating inductive effect (+I) is exhibited by four methyl groups in $\mathbf{1}^{+\bullet}$, and the spin densities in $\mathbf{1}^{+\bullet}$ are predominantly localized within the pyrene and thiophene rings. As expected, the DFT calculation results for $\mathbf{2}^{+\bullet}$ are similar to those for $\mathbf{1}^{+\bullet}$. The lowest unoccupied molecular orbitals (LUMO) and single occupied molecular orbitals (SOMO) of $\mathbf{2}^{+\bullet}$ extend within the maintaining molecule, with less dispersion on the thiophene ring, but significantly prominent in the pyrene region (Figure 5c). The total energy of the two radical cations is very close, -3293.6863 a.u. for $\mathbf{1}^{+\bullet}$ and -3595.6169 a.u. for $\mathbf{2}^{+\bullet}$. Four alkylthienyl groups in $\mathbf{1}^{+\bullet}$ and $\mathbf{2}^{+\bullet}$ show an electron donating inductive effect (+I) and the spin densities in radicals are mainly distributed among the hold rings. Substituents with different polarities lead to a change in the charge recombination free energy (ΔG) while the solvent reorganization energy (λ) remains constant. Those will affect the sign of the electron exchange interaction (J) value. Meanwhile, the J value is defined by the energy separation between singlet and triplet radical pairs. Therefore, substituents with different inductive effects (+I or -I) affect on singlet-triplet energy ordering to determine which the ground state is influencing the J value.

Magnetic properties

Quantification of the electronic coupling interaction between the highly active species was done using SQUID measurements on the solid of radical cations $\mathbf{1}^{+\bullet}$ and $\mathbf{2}^{+\bullet}$ (Figure 6). The molar paramagnetic susceptibility and temperature, $X_m T$, of $\mathbf{1}^{+\bullet}$ were found to be $0.385 \text{ cm}^3 \text{ K mol}^{-1}$ at 298 K, with the maximum value remaining at 90 K upon cooling. It exhibits a progressive decline with increasing temperature reduction from 90 to 0 K (At 2 K, $0.04 \text{ cm}^3 \text{ K mol}^{-1}$), suggesting the presence of an intermolecular interaction (Figure 6a). From 298 to 20 K, $X_m T$ for $\mathbf{2}^{+\bullet}$ was found to be $0.375 \text{ cm}^3 \text{ K mol}^{-1}$ (Figure 6b). From 20 to 2 K, it decreased progressively (at 2 K, $0.10 \text{ cm}^3 \text{ K mol}^{-1}$), although more quickly than $\mathbf{1}^{+\bullet}$, suggesting a weaker connection. The magnitude of intermolecular forces between $\mathbf{1}^{+\bullet}$ and $\mathbf{2}^{+\bullet}$ is related to the electronic effects of substituents at positions 4, 5, 9, and 10 of the pyrene skeleton.

Photophysical properties

It is useful to use UV-Vis spectroscopy to look at the optical properties of radicals.³⁸ In light of the unique magnetism exhibited by compounds $\mathbf{1}$ - $\mathbf{2}$, the UV-Vis absorption spectra of $\mathbf{1}$ - $\mathbf{2}$ and their respective cationic radical species $\mathbf{1}^{+\bullet}$ - $\mathbf{2}^{+\bullet}$ were obtained at ambient temperature in the solid state (Figure 6). As depicted in Figure 6a, the absorption spectrum of compound $\mathbf{1}$ in the solid state exhibited two prominent signals. The transition from π to π^* in the conjugated backbone is responsible for the signal at a longer wavelength, roughly 310-360 nm, while the electronic transitions of the distinct aromatic units are linked to the band at a shorter wavelength, $\lambda_{\text{max}} = 260$ -310 nm. In the solid state, the absorption spectrum of compound $\mathbf{1}$ exhibited a signal at 250 nm, with smaller signals at 285 and 355 nm. The absorption spectrum of the $\mathbf{1}^{+\bullet}$ species displayed similarities to that of compound $\mathbf{1}$ in solution, with three signals concentrated in the 250-380 nm range ($\lambda_{\text{max}} = 265$ nm). Owing to their comparable

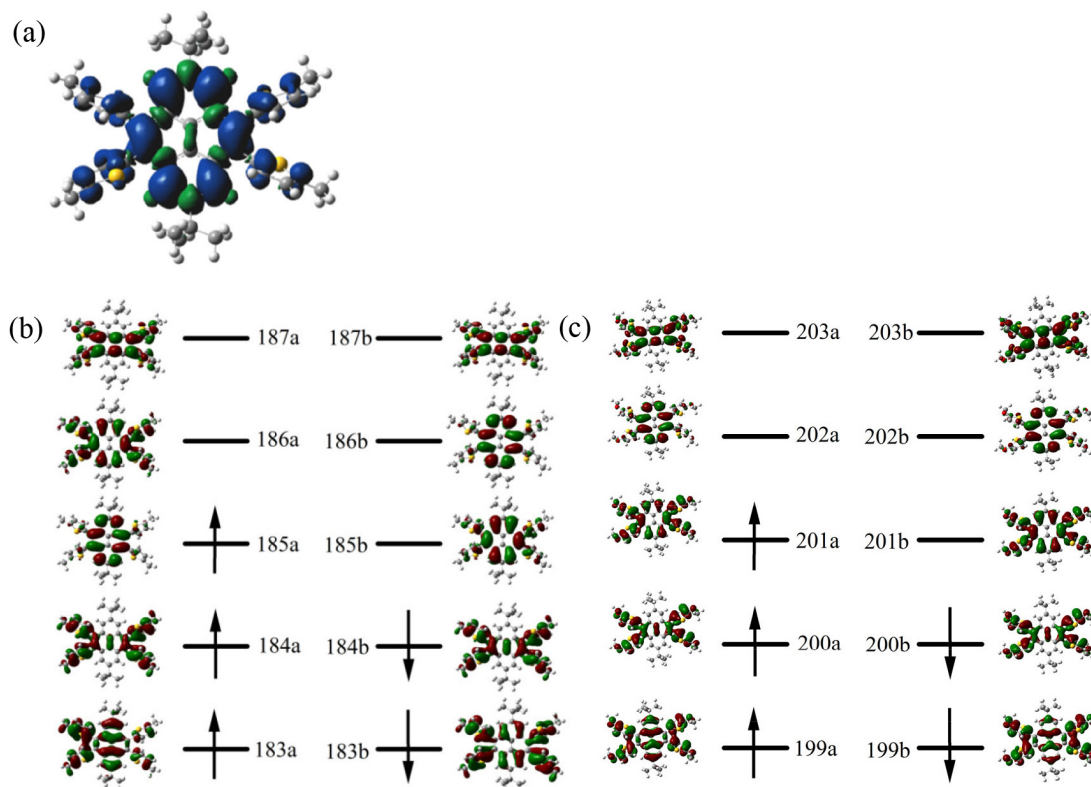


Figure 5. (a) Spin density map of $\mathbf{1}^{+\bullet}$. (b) The SOMO of $\mathbf{1}^{+\bullet}$ and the LUMO of $\mathbf{1}^{+\bullet}$. (c) The SOMO of $\mathbf{2}^{+\bullet}$ and the LUMO of $\mathbf{2}^{+\bullet}$

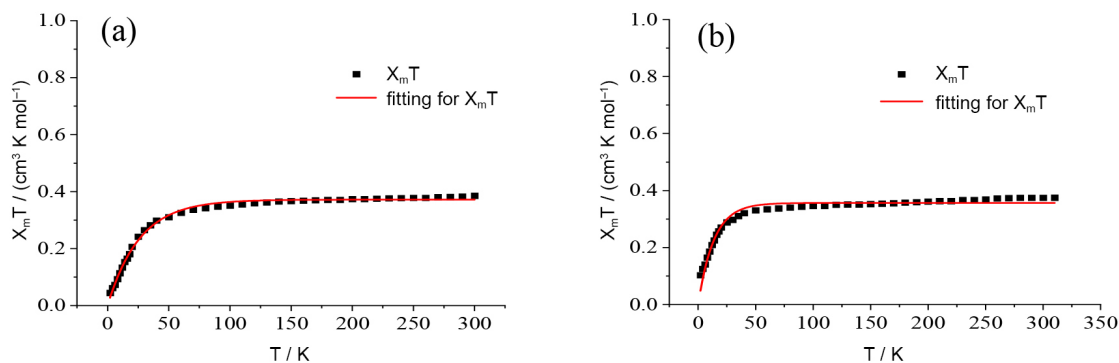


Figure 6. SQUID magnetometry on powder samples (a) 1^{+} , (b) 2^{+} at 1000 Oe in the warming mode

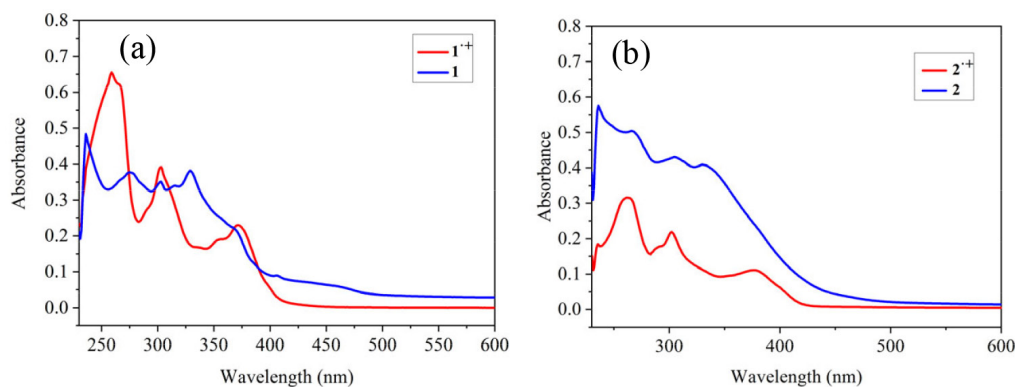


Figure 7. (a) UV absorption spectra of **1** and 1^{+} in solid state, (b) **2** and 2^{+} in solid state

structures, **1** and **2** produced spectral shapes that were almost identical in terms of their features (such as fine structures and narrow, strong maximum signals). Because of the thiophene and other aromatic groups, the conjugated compounds all displayed absorption signals at high level energy (~ 250 nm).³⁹ Additionally, the beginning point of the absorption signals rose by more than 10 nm upon the conversion from **1** to 1^{+} (and **2** to 2^{+}). Free radical compounds are often found to exhibit a little shift towards longer wavelengths in the UV-Vis absorption spectrum when compared to their neutral counterparts. In this investigation, the spectra of **1** and **2** were compared with the spectra of their respective radical forms, 1^{+} and 2^{+} , revealing distinct signals indicative of radical absorption at 405 nm. This finding supports the radical nature of **1** and **2**. The energy difference between the HOMO and LUMO (ΔE_{gap}) was determined from the absorption onset wavelength ($\lambda_{\text{abs-onset}}$) using the formula: $\Delta E_{\text{gap}} = 1240/\lambda_{\text{abs-onset}}$. For **1** and **2**, the $\lambda_{\text{abs-onset}}$ values were 402 and 429 nm, respectively, which led to the calculation of the gaps of 3.08 and 2.82 eV for **1** and **2**. The creation of a more extended and delocalized π -conjugated system is also consistent with this minor decrease of the gap, which is typically found in conjugated oligomers. Compared to 2.5 eV, which is greater than several well-known OFET materials, this gap is much higher. Furthermore, a comparison between **1** and **2** revealed that the gap of **2** was marginally smaller than that of **1** because the $\lambda_{\text{abs-onset}}$ of **2** with a methoxy was larger than that of **1** with a methyl substituent. A wider gap often indicates greater photo-degradation stability.⁴⁰ Due to its larger rigid core, compound **1** demonstrates strong π - π interactions and may serve as a promising material for use in organic electronic devices. Ongoing research is focused on exploring the potential application of this compound in electronic devices such as field effect transistors.

CONCLUSIONS

In summary, we have generated the initial thiophene-modified

pyrene radical cations 1^{+} and 2^{+} via $\text{Ag}[\text{Al}(\text{OC}(\text{CF}_3)_3)_4]$ as the oxidizing agent. Examination through EPR spectroscopy and DFT calculations revealed that these cationic radicals displayed distinct characteristics in comparison to the corresponding neutral thiophene-modified pyrene compounds. Comparing these TTPs to other smaller PAHs, our data reveals an intriguing finding: despite the two distinct substituents of pyrene linked by thiophene, the magnetic/optoelectronic properties of these two TTPs are partially identical. For instance, the inclusion of an electron-rich thiophene group conferred some diradical properties to the one-electron oxidized compounds 1^{+} - 2^{+} . The radical cation 1^{+} exhibits enhanced stability and demonstrates superior optoelectronic characteristics. Furthermore, in contrast to 2^{+} , 1^{+} produces more prominent diradical characteristics at lower temperatures, a reduced $\lambda_{\text{abs-onset}}$, and an increased bandgap. Overall, the bulky group is anticipated to not only enhance the stability of the resulting cation by dispersing electron spin density but also hinder intermolecular electronic interaction to yield a distinct radical. Methoxy has a strong electron-donating ability, which can increase the electron density of the thiophene group connected to the carbon atom and change the strength of the coupling. The steric hindrance of methyl substituents is small and has a certain electron-donating ability, which is beneficial for increasing intermolecular coupling. This work offers a novel way to control the physicochemical parameters and electron spin density distribution of organic radicals. The photoelectric qualities of monoradical cations also point to a wide range of potential uses for them in the realm of novel photoelectric materials.

SUPPLEMENTARY MATERIAL

Some images of the systems used in this work are available in <http://quimicanova.s bq.org.br> as a PDF file, with free access.

ACKNOWLEDGMENTS

The film investigated in this work was fabricated in the Key Laboratory of Functional Molecular Solids of the Ministry of Education, Anhui Normal University. The authors declare that they have no conflict of interest.

REFERENCES

1. Power, P. P.; *Chem. Rev.* **2003**, *103*, 789. [Crossref]
2. Mas-Torrent, M.; Crivillers, N.; Rovira, C.; Veciana, J.; *Chem. Rev.* **2012**, *112*, 2506. [Crossref]
3. Joo, Y.; Agarkar, V.; Sung, S. H.; Savoie, B. M.; Boudouris, B. W.; *Science* **2018**, *359*, 1391. [Crossref]
4. Phan, H.; Herng, T. S.; Wang, D.; Li, X.; Zeng, W.; Ding, J.; Loh, K. P.; Wee, A. T. S.; Wu, J.; *Chem* **2019**, *5*, 1223. [Crossref]
5. Tan, Y.; Hsu, S. N.; Tahir, H.; Dou, L.; Savoie, B. M.; Boudouris, B. W.; *J. Am. Chem. Soc.* **2022**, *144*, 626. [Crossref]
6. Harvey, S. M.; Wasielewski, M. R.; *J. Am. Chem. Soc.* **2021**, *143*, 15508. [Crossref]
7. Steelman, M. E.; Adams, D. J.; Mayer, K. S.; Mahalingavelar, P.; Liu, C. T.; Eedugurala, N.; Lockart, M.; Wang, Y.; Gu, X.; Bowman, M. K.; Azoulay, J. D.; *Adv. Mater.* **2022**, *34*, 1. [Crossref]
8. Ai, X.; Evans, E. W.; Dong, S.; Gillett, A. J.; Guo, H.; Chen, Y.; Hele, T. J. H.; Friend, R. H.; Li, F.; *Nature* **2018**, *563*, 536. [Crossref]
9. Han, H.; Zhang, D.; Zhu, Z.; Wei, R.; Xiao, X.; Wang, X.; Liu, Y.; Ma, Y.; Zhao, D.; *J. Am. Chem. Soc.* **2021**, *143*, 17690. [Crossref]
10. Li, D.; Song, J.; Yin, P.; Simotwo, S.; Bassler, A. J.; Aung, Y.; Roberts, J. E.; Hardcastle, K. I.; Hill, C. L.; Liu, T.; *J. Am. Chem. Soc.* **2011**, *133*, 14010. [Crossref]
11. Jiao, D.; Geng, J.; Loh, X. J.; Das, D.; Lee, T. C.; Scherman, O. A.; *Angew. Chem., Int. Ed.* **2012**, *51*, 9633. [Crossref]
12. Ni, X. L.; Wang, S.; Zeng, X.; Tao, Z.; Yamato, T.; *Org. Lett.* **2011**, *13*, 552. [Crossref]
13. Kim, J. S.; Quang, D. T.; *Chem. Rev.* **2007**, *107*, 3780. [Crossref]
14. Duarte, T. M. F.; Müllen, K.; *Chem. Rev.* **2011**, *111*, 7260. [Crossref]
15. Feng, X.; Hu, J. Y.; Redshaw, C.; Yamato, T.; *Chem. - Eur. J.* **2016**, *22*, 11898. [Crossref]
16. Werder, S.; Malinovskii, V. L.; Häner, R.; *Org. Lett.* **2008**, *10*, 2011. [Crossref]
17. Kowser, Z.; Rayhan, U.; Akther, T.; Redshaw, C.; Yamato, T.; *Mater. Chem. Front.* **2021**, *5*, 2173. [Crossref]
18. Shi, Y. R.; Wei, H. L.; Shi, Y. T.; Liu, Y. F.; *Synth. Met.* **2017**, *223*, 218. [Crossref]
19. Venkataramana, G.; Sankararaman, S.; *Eur. J. Org. Chem.* **2005**, *2005*, 4162. [Crossref]
20. Didane, Y.; Mehl, G. H.; Kumagai, A.; Yoshimoto, N.; Vidélot-Ackermann, C.; Brisset, H.; *J. Am. Chem. Soc.* **2008**, *130*, 17681. [Crossref]
21. Li, M.; Zheng, J.; Wang, X.; Yu, R.; Wang, Y.; Qiu, Y.; Cheng, X.; Wang, G.; Chen, G.; Xie, K.; Tang, J.; *Nat. Commun.* **2022**, *13*, 4912. [Crossref]
22. Park, S.; Choi, W.; Kim, S. H.; Lee, H.; Cho, K.; *Adv. Mater.* **2023**, *35*, 2303707. [Crossref]
23. Xu, X.; Megarajan, S. K.; Zhang, Y.; Jiang, H.; *Chem. Mater.* **2020**, *32*, 3. [Crossref]
24. Roncali, J.; Leriche, P.; Blanchard, P.; *Adv. Mater.* **2014**, *26*, 3821. [Crossref]
25. Zeng, Z.; Shi, X.; Chi, C.; Navarrete, J. T. L.; Casado, J.; Wu, J.; *Chem. Soc. Rev.* **2015**, *44*, 6578. [Crossref]
26. Yamato, T.; Miyazawa, A.; Tashiro, M.; *Chem. Ber.* **1993**, *126*, 2505. [Crossref]
27. Miura, Y.; Yamano, E.; *J. Org. Chem.* **1995**, *60*, 1070. [Crossref]
28. Stille, J. K.; *Angew. Chem., Int. Ed.* **1986**, *25*, 508. [Crossref]
29. Wilson, P.; Lacey, D.; Sharma, S.; *Mol. Cryst. Liq. Cryst.* **2001**, *368*, 279. [Crossref]
30. Duan, Z. F.; Yang, Z. G.; Liu, D. J.; Cai, L.; Hoshino, D.; Morita, T.; Zhao, G. Y.; Nishioka, Y.; *Chin. Chem. Lett.* **2011**, *22*, 819. [Crossref]
31. Duan, Z. F.; Huang, X. Q.; Yang, Z. G.; Hoshino, D.; Kitanaka, S.; Zhao, G. Y.; Nishioka, Y. A.; *Molecules* **2011**, *16*, 4467. [Crossref]
32. Duan, Z. F.; Hoshino, D.; Yang, Z. G.; Yano, H.; Ueki, H.; Liu, Y. W.; Ohuchi, H.; Takayanagi, Y.; Zhao, G. Y.; Nishioka, Y.; *Mol. Cryst. Liq. Cryst.* **2011**, *538*, 199. [Crossref]
33. Dong, X.; Chen, M.; Wang, R.; Ling, Q.; Hu, Z.; Liu, H.; Xin, Y.; Yang, Y.; Wang, J.; Liu, Y.; *Adv. Energy Mater.* **2023**, *13*, 2301006. [Crossref]
34. Sun, Q.; Wang, H.; Yang, C.; Li, Y.; *J. Mater. Chem.* **2003**, *13*, 800. [Crossref]
35. Tang, M. L.; Reichardt, A. D.; Wei, P.; Bao, Z. N.; *J. Am. Chem. Soc.* **2009**, *131*, 5264. [Crossref]
36. Porzio, W.; Destri, S.; Giovannella, U.; Pasini, M.; Marin, L.; Iosip, M. D.; Campione, M.; *Thin Solid Films* **2007**, *515*, 7318. [Crossref]
37. Grimme, S.; Hansen, A.; Brandenburg, J. G.; Bannwarth, C.; *Chem. Rev.* **2016**, *116*, 5105. [Crossref]
38. Kirmse, W.; Kilian, J.; *J. Am. Chem. Soc.* **1990**, *112*, 6400. [Crossref]
39. Vidélot-Ackermann, C.; Ackermann, J.; Kawamura, K.; Yoshimoto, N.; Brisset, H.; Raynal, P.; Kassmi, A. E.; Fages, F.; *Org. Electron.* **2006**, *7*, 465. [Crossref]
40. Meng, H.; Sun, F.; Goldfinger, M. B.; Jaycox, G. D.; Li, Z.; Marshall, W. J.; Blackman, G. S.; *J. Am. Chem. Soc.* **2005**, *127*, 2406. [Crossref]

